Biochemical and Biophysical Research Communications **267,** 156–163 (2000)
doi:10.1006/bbrc.1999.1926, available online at http://www.idealibrary.com on IDEAL®

Cloning of the β_{2a} Subunit of the Voltage-Dependent Calcium Channel from Human Heart: Cooperative Effect of α_2/δ and β_{2a} on the Membrane Expression of the α_{1C} Subunit

Hiroshi Yamaguchi,*,[1] Masaru Okuda,† Gabor Mikala,*,[2] Kenji Fukasawa,† and Gyula Varadi*,†,[3]
Institute of Molecular Pharmacology and Biophysics and †Department of Cell Biology, Neurobiology, and Anatomy, University of Cincinnati, College of Medicine, 231 Bethesda Avenue, Cincinnati, Ohio 45267-0828

Received November 14, 1999

Expression and membrane localization of an epitope-tagged human Ca^{2+} channel α_{1C} subunit were monitored in *Xenopus* oocytes by confocal microscopy and electrophysiological recording. When α_2/δ and β_{2a} were separately coexpressed with the α_{1C} subunit, assessment by confocal microscopy showed an 86 and 225% increase of the channel density, respectively. Simultaneous coexpression of α_2/δ and β_{2a} subunits resulted in a cooperative (470%) increase. Electrophysiological measurements performed in parallel revealed that the current augmentation by the α_2/δ subunit is totally attributable to an increase in channel density, whereas the β_{2a} subunit, in addition to increasing channel density, also facilitates channel opening.

Voltage-dependent calcium channels (VDCC) play a pivotal role in the entry of Ca^{2+} into cells thereby activating various downstream biological activities. It is believed that the principal, pore-forming α_1 subunit as well as the auxiliary α_2/δ, β, and sometimes γ subunits comprise the native high-voltage-activated Ca^{2+} channel holocomplex [for reviews see (1–3)]. Profound modulatory effects of the α_2/δ subunit (4–12) and β subunits (4, 6–8, 12–33) on channel function have been well documented. It is generally accepted that these auxiliary subunits increase the amplitude of currents through the formation of the holocomplex (3). However, the mechanism(s) of current augmentation when auxiliary subunits are coexpressed remains controversial. Two distinct mechanisms have been proposed: increased channel number in the plasma membrane and/or increased channel opening. In terms of channel density, some studies show that the α_2/δ subunit increases ligand binding sites (5, 11), channel protein (6), and gating currents (9, 12). In other studies (8, 10), ligand binding sites were found unchanged by α_2/δ coexpression. In support of the latter, no effect was detected on membrane targeting of the α_{1A} (29) and the α_{1C} subunit (33) by the α_2/δ subunit when monitored by an immunohistochemical method.

Similarly, upon coexpression with β subunits, an increased number of ligand binding sites (14, 15, 20), gating currents (12, 26, 27), membrane expression of the channel complex (25, 29, 32) was observed. This suggests an increased amount of channel protein in the plasma membrane. In contrast, in other studies, no change was reported in ligand binding sites (22), gating currents (17), or channel protein (6, 19) when coexpressed with the β subunit. These inconsistencies may be ascribed to the difference in the expression system used or perhaps to different targeting by different subunit isoforms. Further, some of the previously measured parameters do not necessarily reflect the channel amount in the plasma membrane. It is possible that the number of ligand binding sites may be altered by allosteric modulation of the channel (1). Gating currents do not necessarily reflect channel number accurately (34), since it is known that many

The nucleotide sequence reported in this paper has been submitted to the GenBank/EBI Data Bank and has Accession No. AF137377.

Abbreviations used: HA, influenza virus hemagglutinin; CLSM, confocal laser-scanning microscopy; PCR, polymerase chain reaction; V_{mid}, midpoint potential.

[1] Present address: 3rd Department of Internal Medicine, Chiba University School of Medicine, 1-8-1 Inohana, Chuo-Ku, Chiba 260-8670, Japan.

[2] Present address: Division of Clinical Pharmacology, 1st Department of Internal Medicine, Haynal Imre University of Health Sciences, 35 Szabolcs St., Budapest, H-1135, Hungary.

[3] To whom correspondence should be addressed. Fax: (513) 558-1778. E-mail: varadig@email.uc.edu.

0006-291X/00 $35.00

```
humanβ2a  M-----------------------------------QCC----------GLVHRRRVR----------------VS  ( 15)
ratβ2a    M-----------------------------------***----------*********----------------**  ( 15)
rabbitβ2a M-----------------------------------LDR----------H*AAPHTQGL----------------*L  ( 16)
rabbitβ2b M-----------------------------------NQASGLDLLKISY*KGA**KN*FKGSDGSTSSDTTSNSF*R  ( 42)
humanβ2c  MVQRDMSKSPPTAAAAVAQEIQMELLENVAPAGALGAAA*SY----------*KGA**KN*----------------FK  ( 53)
mouseβ2d  M-----------------------------------KAT----------WIRLLK*AK----------------GG  ( 15)

humanβ2a  Y----------------GSADSYTSRPSDSDVSLEEDREAVRREAERQAQAQLEKAKTKPVAFAVRTNVSYSAAHEDDV  ( 78)
ratβ2a    *----------------**************************************************R****Q****  ( 78)
rabbitβ2a E----------------**************************************************************  ( 79)
rabbitβ2b Q----------------**************************************************************  (105)
humanβ2c  GSDGSTSSDTTSNSFLRQ**************************-Q******************D**********  (132)
mouseβ2d  RLKSSDIC----------**************************************************R***RQ****  ( 85)
```

FIG. 1. N-terminal amino acid sequence alignments for human cardiac β_{2a} (this paper), β_{2c} (34), rat cardiac/brain β_{2a} (16), rabbit cardiac β_{2a}, β_{2b} (44), and mouse β_{2d} (45) subunits. "*" stand for conserved amino acid residues, "−" for alignment gaps. Consensus palmitoylation sites are shown in boldface.

drugs and toxins can alter the gating currents in voltage gated channels. For example, in L-type calcium channels, gating currents are decreased by dihydropyridines (35, 36). Thus it is possible that allosteric or cooperative mechanisms may explain how the auxiliary subunits affect gating currents, and therefore influence the channel number.

We have shown that the modulatory effects of the β_3 subunit on the α_{1C} subunit are mediated by both trafficking and allosteric modulation of the channel complex (32). In the present study we seek conclusive evidence as to whether the α_2/δ subunit and the palmitoylation-competent β_{2a} subunit increase membrane expression of the channel complex individually and in combination. Electrophysiological measurements performed in parallel allow the assessment of the relative contribution of channel expression and/or allosteric modulation by the auxiliary subunits.

MATERIALS AND METHODS

Cloning of β_{2a} subunit cDNA from the human heart. Cloning of one isoform of the β_2 subunit family from human heart, β_{2c}, has been reported (37). We sought for molecular evidence as to whether a β_{2a}-type isoform exists in human heart. We employed reverse-transcription PCR from human heart RNA with the following primers: 5′-ATGCAGTGCTGCGGGCTGGTAC-3′ and 5′-TTTGCTTC-GAATGAGATGGC-3′. A short PCR product that encodes the alternatively spliced N-terminal region was generated (265 bp) upon amplification using Vent DNA polymerase (New England Biolabs). The PCR product was subcloned into the *Eco*RV site of pBluescriptII and sequenced. To obtain a full-length clone, the rest of the human β_{2a} sequence was taken from the human β_{2c} (37) clone by restriction cleavage (*Hin*dIII and *Bst*BI) followed by ligation of the appropriate pieces.

Expression of calcium channel subunits and electrophysiological recordings. An HA epitope was introduced to the N-terminus of the human heart L-type calcium channel α_{1C} subunit (38) as described previously (32). Capped cRNAs were synthesized from the HA-tagged α_{1C} subunit, α_2/δ subunit (39), and the human heart β_{2a} subunit cDNAs as templates using the mMESSAGE mMACHINE *in vitro* transcription kit (Ambion). Preparation of *Xenopus laevis* oocytes, microinjection of cRNAs, and electrophysiological recordings were done as described previously (32, 40).

Immunohistochemical study. Oocytes expressing calcium channel subunits were fixed in 3.7% formaldehyde, 0.25% glutaraldehyde, and permeabilized with 0.2% Triton X-100 at room temperature. Oocytes were then postfixed in 100% methanol at −20°C overnight, incubated with 2% bovine serum albumin for 1 h at room temperature, followed by incubation with 10 μg/ml fluorescein-conjugated anti-HA monoclonal antibody (Boehringer-Mannheim) at 4°C overnight. Finally, the oocytes were washed extensively in PBS, and examined by CLSM.

Confocal images were collected using a microscope (Nikon) equipped with a confocal laser scanning unit (MRC-600, Bio-Rad), a 25-mW argon ion laser, and a 10× objective lens (Nikon). Fluorescence was excited using the 488-nm laser line and collected through a fluorescein isothiocyanate filter (530 nm). Acquired images were imported into CoMOS software (Bio-Rad) for measurement of the signals and image processing.

For quantitative measurement of channel amount, a z section at the equator of oocytes was Kalman averaged for six times, and pixel intensity (8 bit, 0–256) was measured along ten straight lines that were randomly drawn right-angled to the animal pole side of oocyte plasma membrane. The integral of pixel intensity along ten lines was considered to represent the channel density in the plasma membrane of each oocyte. The power of laser, photomultiplier gain, and black level were always kept constant. It was confirmed that pixels were not saturated.

Statistical analyses. Unpaired *t* tests were performed for comparing average values. A value of $p < 0.05$ was considered as statistically significant difference.

RESULTS

Cloning of the β_{2a} subunit from the human heart. Although there has been experimental evidence presented for the lack of the palmitoylated β_{2a} isoform in rabbit heart (41), our RT-PCR strategy to isolate a rat β_{2a}-like (palmitoylation-competent) sequence from human heart RNA was successful. The human β_{2a} subunit was expressed in *Xenopus* oocytes, and was shown to be fully functional. The isolated and sequenced clone segment shows 100% amino acid homology with the respective rat β_{2a} region, including the expected palmitoylation site at the very N-terminus and a shorter N-terminal domain as compared to β_{2b} and β_{2c} (Fig. 1). The actual amino acid identities of the full-length clones are (based on the human β_{2a}): ratβ_{2a}, 93.9%;

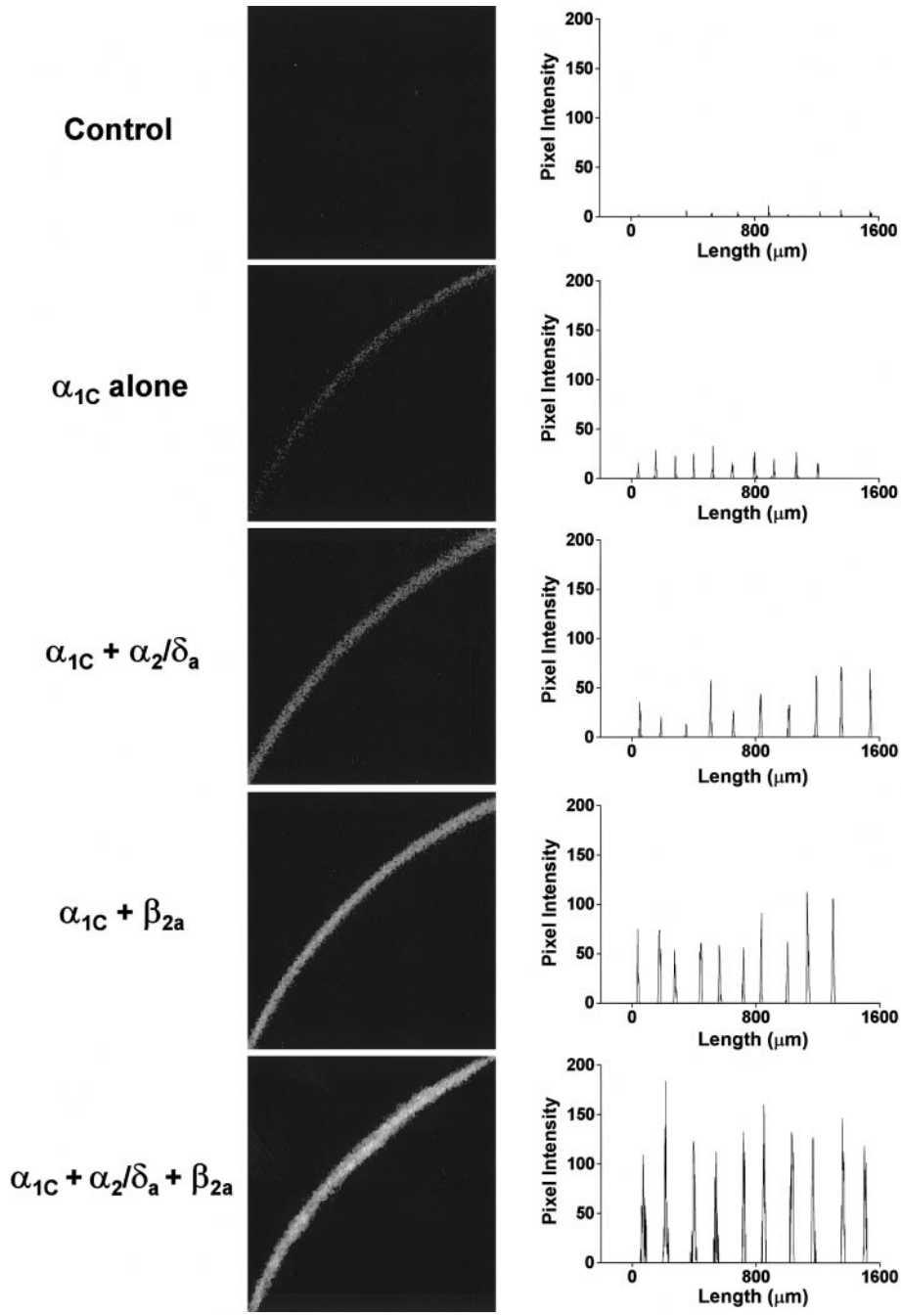

FIG. 2. Immunofluorescence detection of the channel complex in oocyte plasma membrane. Oocytes were stained with fluorescein-conjugated anti-HA antibody and analyzed by CLSM. (Left panels) Representative confocal images at the equator of each oocyte for different subunit combinations. (Right panels) Corresponding pixel intensities measured along ten straight lines randomly drawn right-angled to the plasma membrane. Oocytes shown in this figure were derived from the same series of experiment.

rabbitβ_{2a}, 94.7%; rabbitβ_{2b}, 95.2%; humanβ_{2c}, 97.9%; mouseβ_{2d}, 91.6%.

Coexpression of α_2/δ and β_{2a} cooperatively increases the membrane expression of the α_{1C} subunit. An HA epitope-tagged α_{1C} subunit protein expressed in the oocyte plasma membrane was readily detected by CLSM after being stained with the fluorescein-conjugated anti-HA monoclonal antibody (Fig. 2, left panels). Corresponding measurements of the pixel intensities are shown in Fig. 2, right panels. The background fluorescence that arises from nonspecific binding of the antibody was very low under our experimental conditions. When the α_{1C} subunit was expressed alone, we observed relatively low fluores-

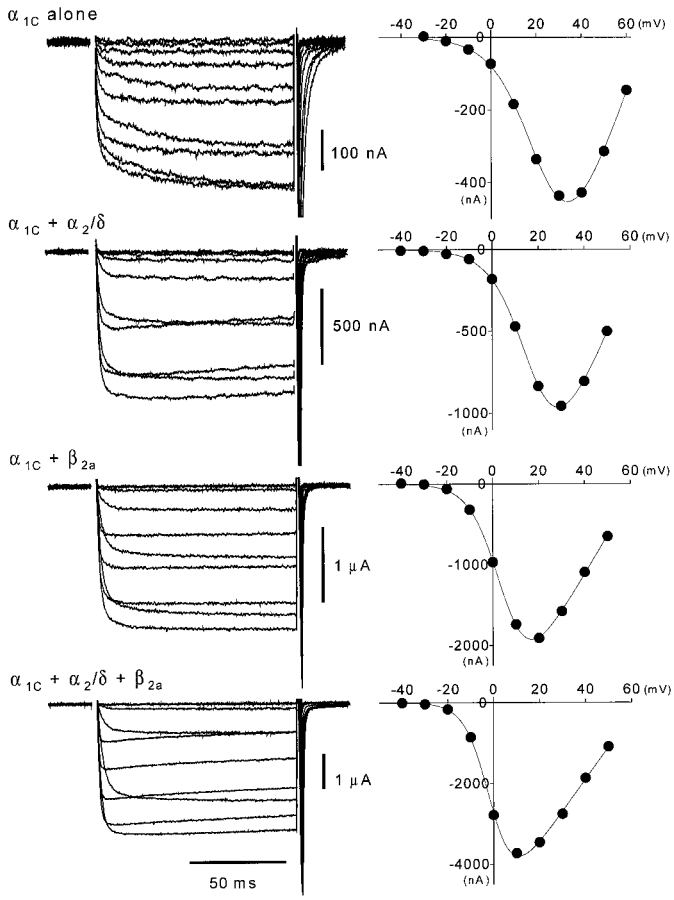

FIG. 3. Representative Ba^{2+} current traces and corresponding current–voltage relationships. Currents were elicited by ten 100-ms depolarizing pulses between −30 and +60 mV (α_{1C} subunit alone) or −40 and +50 mV (other subunit combinations) in 10-mV increments from a holding potential of −80 mV.

cence from the membrane. The integral of pixel intensity was 637 ± 125 (pixel intensity × pixel count, n = 13). Coexpression of the α_2/δ or the β_{2a} with α_{1C} significantly increased the fluorescence. The integral of pixel intensity increased to 1188 ± 216 (n = 12, 86% increase from α_{1C} subunit alone), and 2073 ± 356 (n = 10, 225% increase from α_{1C} subunit alone) when the α_2/δ and β_{2a} subunits were individually coexpressed, respectively. When both the α_2/δ and β_{2a} subunits were simultaneously coexpressed with α_{1C}, a cooperative (i.e., synergistic) increase in fluorescence was observed. The integral of pixel intensity was 3633 ± 578 (n = 11, 470% increase from α_{1C} subunit alone). These results are summarized in Fig. 4A.

Effect of auxiliary subunit coexpression on the characteristics of currents. When expressed alone, the α_{1C} subunit readily gave measurable currents that peaked between +30 and +40 mV. The peak current amplitude was 342 ± 121 nA (n = 9) (Fig. 3, left panels). Coexpression of the accessory subunits increased the current amplitude and shifted the peak current potential to a hyperpolarized direction (Fig. 3, right panels). The α_2/δ subunit increased the averaged peak current to 682 ± 230 nA (n = 10, 99% increase from α_{1C} subunit alone). The current peaked around +30 mV for this subunit combination. β_{2a} subunit coexpression induced a greater effect on the current amplitude, with the average peak current amplitude of 2219 ± 303 nA (n = 12, 548% increase). The peak current potential shifted to +10–20 mV. Finally, coexpression of all three subunits (α_{1C}, α_2/δ, and β_{2a} subunit) resulted in a very large peak current amplitude, 3858 ± 1022 nA (n = 10, 1027% increase). The peak current amplitude was also most shifted by this combination, with currents peaking around +10 mV.

The averaged peak current amplitudes are summarized in Fig. 4B. For a comparison between the channel density (based on the integral of pixel intensity) and the peak current amplitude, the values were normalized to the average value for the α_{1C} subunit alone, and shown as a percent increase (Fig. 4C). Peak current amplitude and channel density were increased to a similar degree by coexpression of the α_2/δ subunit (99 and 86%, respectively). When the β_{2a} subunit was coexpressed with the α_{1C}, the increase of current amplitude was approximately twofold greater than the increase in channel density (548 and 225% increase, respectively). When both the α_2/δ and β_{2a} subunits were coexpressed with the α_{1C} subunit, the channel density and current amplitude exhibited a further increase. However, the ratio between the increase in current amplitude and channel density was still about the same (1027 and 470% increase, respectively).

Effect of the auxiliary subunits on voltage-dependence of activation was also examined (Fig. 5A and Table 1). For the α_{1C} subunit alone, the midpoint potential (V_{mid}) for activation was 22.6 ± 1.1 mV (n = 8). Coexpression of the α_2/δ subunit shifted the V_{mid} for activation to a hyperpolarized direction to 16.3 ± 1.6 mV (n = 8, −6.3 mV shift). The β_{2a} subunit caused a more drastic shift of the V_{mid} for activation to 3.1 ± 1.1 mV (n = 12, −19.5 mV shift). These effects were additive when both the α_2/δ and the β_{2a} subunits were coexpressed with the α_{1C} subunit. The V_{mid} for activation was −2.1 ± 1.8 mV (n = 9, −24.7 mV shift) for this subunit combination. The slope of the steady-state activation curve was increased by the auxiliary subunit coexpression (Fig. 5A and Table 1), and this effect was also additive rather than synergistic.

Coexpression of the α_2/δ subunit with the α_{1C} subunit caused a small but significant shift of the V_{mid} for inactivation without changing the slope of the curve (Fig. 5B and Table 1). The V_{mid} for inactivation was −9.4 ± 1.6 mV (n = 8) for the α_{1C} subunit alone, and was −1.9 ± 2.4 mV (n = 7) for the α_{1C} plus α_2/δ subunit. The β_{2a} subunit, when coexpressed with or without the α_2/δ subunit, increased the slope of the steady-state

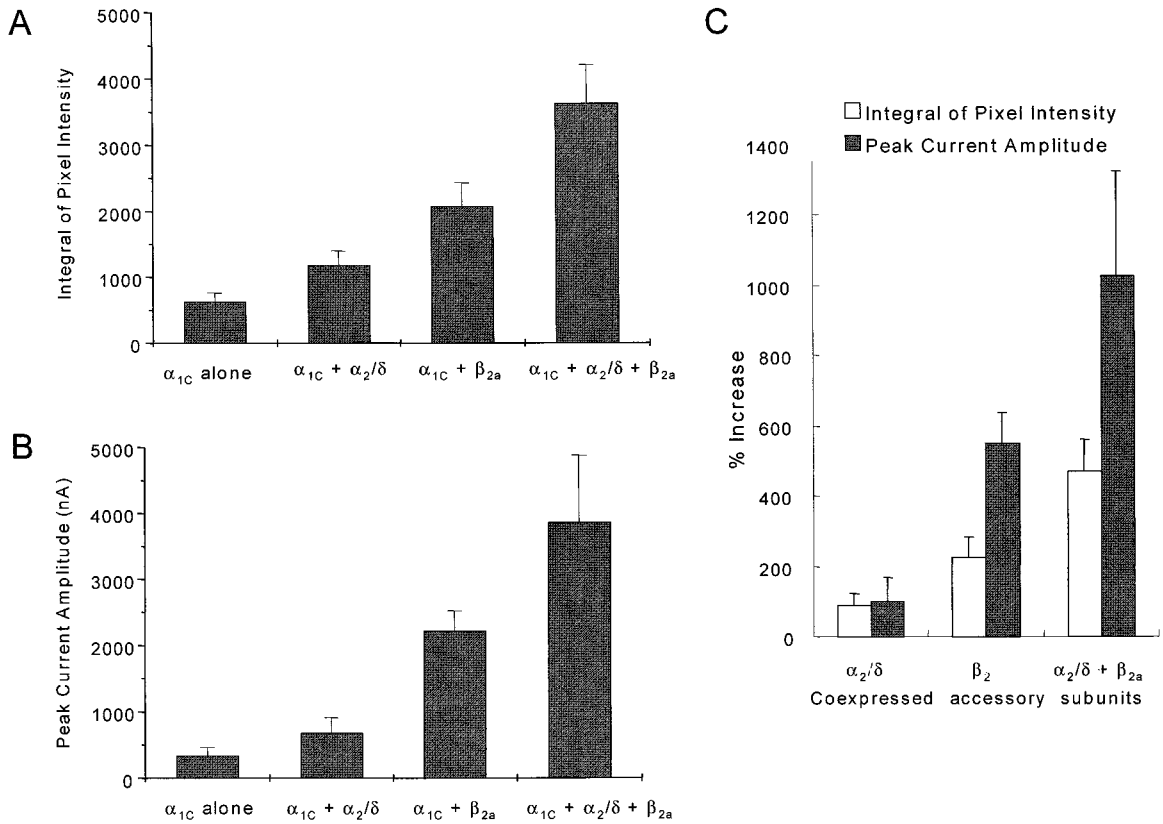

FIG. 4. Summary of the channel density and the peak current amplitude for different subunit combinations. (A) Channel densities (integral of pixel intensity measured and analyzed by using CLSM) in the oocyte plasma membrane. Data are means ± SE from 10 to 13 experiments for each subunit combination. (B) Peak current amplitude for each subunit combination. Data are means ± SE from 9 to 12 experiments. (C) Effects of auxiliary subunit coexpression on the channel density and the peak current amplitude. Values are expressed as percentage increases from α_{1C} subunit alone.

inactivation curve. However, we observed no significant change in the V_{mid} for inactivation.

DISCUSSION

We found that the α_2/δ subunit and the β_{2a} subunit individually are capable of increasing membrane expression of the α_{1C} subunit. Of considerable interest, when both the α_2/δ and the β_{2a} subunits were coexpressed, the increase in channel expression level was cooperative and synergistic rather than additive. The combination α_2/δ and the β_{2a} subunits resulted in 86 and 225% increase of channel expression, respectively. When these two auxiliary subunits were coexpressed with α_{1C}, a remarkable increase of 470% was observed. From these results we suggest that (i) coexpression of the α_2/δ subunit doubles the membrane expression of the α_{1C} subunit and/or the α_{1C}–β_{2a} subunit complex and (ii) the β_{2a} subunit triples the membrane expression of the α_{1C} subunit and/or α_{1C}–α_2/δ subunit complex. Considering that α_2/δ and β subunits bind to the α_1 subunit on distinct sites, it is likely that the two auxiliary subunits increase membrane expression of the channel complex by different mechanisms. Felix *et al.* (11) reported that extracellular α_{1C}–α_2 interaction is responsible for the increased membrane expression. Likewise, it has recently been suggested that the binding of the conserved β-interaction domain to the I–II loop (AID) of the α_1 subunit is responsible for the translocation of the channel complex to the plasma membrane (33, 42). Thus, it seems reasonable that when both α_2/δ and β_{2a} subunit molecules bind to an α_{1C} subunit and form a trimer, two accessory subunits exert the trafficking effect independently, eventually resulting in a cooperative action.

The extent of increase in channel density and current amplitude elicited by the α_2/δ subunit coexpression was comparable, suggesting that the Ca^{2+} current augmentation is entirely attributable to an increase in channel density. This is in agreement with the report by Jones *et al.* (12). In contrast, the β_{2a} subunit increased current amplitude twice the increase that the β_{2a} subunit elicited in channel density, either in the presence or absence of the α_2/δ subunit. This is consistent with single channel studies that showed the β subunit increasing channel opening (6, 21) and with

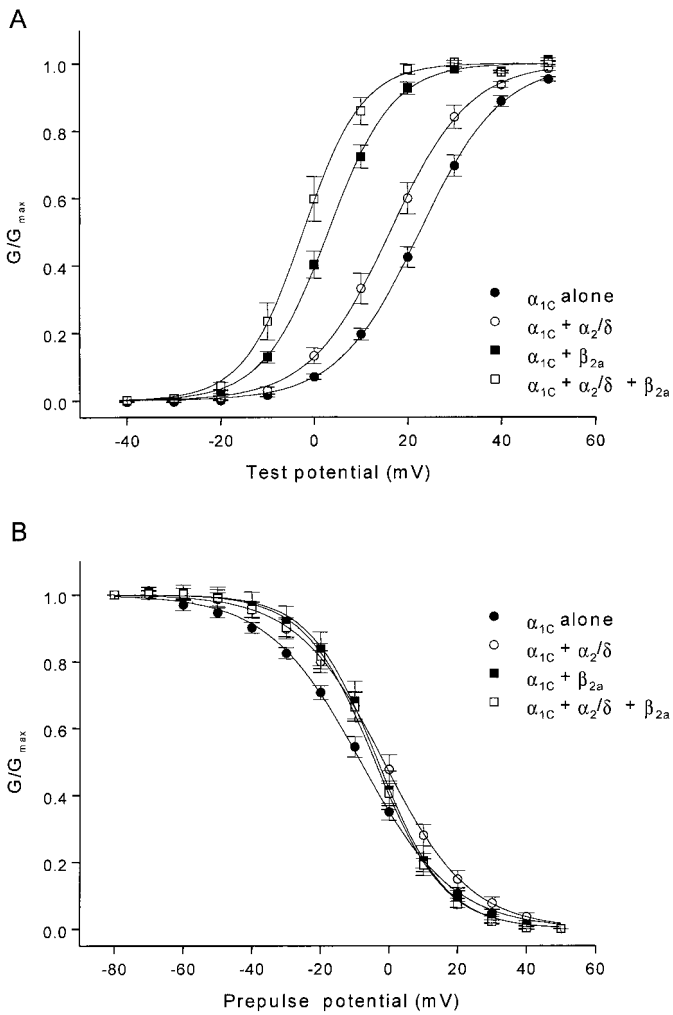

FIG. 5. Voltage-dependence of the channels in different subunit combinations. (A) Steady-state activation curves. Fraction of activated channels were calculated by fitting individual experiments to the equation: $I = G_{max}(V_m - V_{rev})/(1 + \exp(V_{0.5} - V_m)/k)$, where G_{max} is the maximum conductance; V_m, the test potential; V_{rev}, the current reversal potential; $V_{0.5}$, the half-activation potential; k, the slope factor. The curves show Boltzmann distributions that best fitted the averaged data. Means and SE from 8 to 12 experiments for each subunit combination are shown. (B) Steady-state inactivation curves. Inactivated fraction was determined by using a two-pulse protocol in which a 10-s prepulse to indicated potentials was followed by a test pulse to peak current potential. Data are means ± SE from 7 to 9 experiments for each subunit combination. The curves show Boltzmann distributions that best fitted the averaged data.

our previous study using a protein transport inhibitor (32). Interestingly, gating current measurements using identical subunit combinations in the same expression system (17) revealed no increase in gating charge upon β_{2a} coexpression. Consequently, Ca^{2+} channel current increase was explained by an allosteric modulation. In an alternate model (43), it was assumed that palmitoylated β subunits acted solely by an allosteric effect, while all other, nonpalmitoylated β subunits act via dual pathways. Our present results indicate that even if a palmitoylation-competent β subunit is used, part of the current augmentation is due to enhanced surface expression of Ca^{2+} channels.

The α_2/δ subunit and the β_{2a} subunit shifted the voltage-dependence of activation of the channel to a hyperpolarized direction but to a different extent. The shift of the V_{mid} for activation caused by the β_{2a} subunit was much greater than that caused by the α_2/δ subunit. Presumably the binding of these auxiliary subunits modifies the conformation of the channel complex and decreases the energy barrier for channel opening. Our data show that when both the α_2/δ and β_{2a} subunits are coexpressed with the α_{1C} subunit the shift of the V_{mid} for activation is explained by simple addition of two separate effects. Furthermore, the increase in slope of the steady-state activation curves by the auxiliary subunits was also additive. From these results it is likely that individual binding of the α_2/δ and the β_{2a} subunits to the α_{1C} subunit causes different conformational changes unique to the accessory subunit, and these conformational changes are observed as additive effects in terms of the voltage-dependence of activation.

Previous reports showed large, subtype-specific effects of accessory subunits on the voltage-dependent inactivation (4, 12, 23). In the present study the auxiliary subunits evoked relatively small changes in the voltage-dependence of inactivation. The coexpression of α_2/δ subunit shifted the V_{mid} for inactivation 7.5 mV to a depolarized direction. This effect was "canceled" by additional coexpression of the β_{2a} subunit. The V_{mid} for inactivation was not significantly different from α_{1C} subunit alone for $\alpha_{1C} + \alpha_2/\delta + \beta_{2a}$ or $\alpha_{1C} + \beta_{2a}$ subunit combination. Additionally, the slope of the steady-state inactivation curve was increased by the β_{2a} subunit regardless of the existence of the α_2/δ subunit.

The coupling between voltage-dependent activation and inactivation became tighter by coexpression of auxiliary subunits. The difference between the V_{mid} for activation and inactivation, as a measure of coupling, was α_{1C} (32.0 mV) > $\alpha_{1C} + \alpha_2/\delta$ (18.2 mV) > $\alpha_{1C} + \beta_{2a}$ (7.3 mV) > $\alpha_{1C} + \alpha_2/\delta + \beta_{2a}$ (3.4 mV) suggesting that in the absence of the auxiliary subunits, a higher fraction of channels inactivate without opening. The α_2/δ and the β_{2a} subunits cooperatively restore the tight coupling and thus improve the efficiency of channels to permeate ions.

In conclusion, our findings definitively show that the α_2/δ and the β_{2a} subunits cooperatively increase the membrane expression of the α_{1C} subunit whereas their effects on the voltage-dependence of the channel complex are additive. Moreover, the β_{2a} subunit, but not the α_2/δ subunit, enhances the efficiency of the channel to open.

TABLE 1

Voltage Dependence of Activation and Inactivation

	Activation			Inactivation		
	V_{mid} (mV)	Slope (mV)	*n*	V_{mid} (mV)	Slope (mV)	*n*
α_{1C} alone	22.6 ± 1.1	8.5 ± 0.1	8	−9.4 ± 1.6	13.7 ± 0.5	8
$\alpha_{1C} + \alpha_2/\delta$	16.3 ± 1.6	8.1 ± 0.3	8	−1.9 ± 2.4	12.5 ± 0.5	7
$\alpha_{1C} + \beta_{2a}$	3.1 ± 1.1	6.5 ± 0.2	12	−4.2 ± 2.3	10.3 ± 1.2	9
$\alpha_{1C} + \alpha_2/\delta + \beta_{2a}$	−2.1 ± 1.8	5.5 ± 0.3	9	−5.5 ± 1.9	10.3 ± 0.8	8

Note. Current–voltage relationships and current–prepulse voltage relationships were individually fitted to Boltzmann distributions to derive values for the midpoint (V_{mid}) and the slope (mV/*e*-fold change in G/G_{max}) of the curves. The prepulses were 10 s long. Data represent means ± SE. Underlining indicates statistically significant differences from values for the α_{1C} subunit alone, with $P < 0.05$.

ACKNOWLEDGMENTS

We thank Dr. Arnold Schwartz for encouraging this work and critically reading the manuscript. This work was supported in part by American Heart Association Ohio–West Virginia Affiliate Postdoctoral Fellowship SW-97-35-F (to H.Y.), by a grant from The Naito Foundation (to H.Y.), and by National Institute of Health Grant PO1 HL22619-21.

REFERENCES

1. Catterall, W. A. (1995) *Annu. Rev. Biochem.* **64,** 493–531.
2. Varadi, G., Mori, Y., Mikala, G., and Schwartz, A. (1995) *Trends Pharmacol. Sci.* **16,** 43–49.
3. Walker, D., and De Waard, M. (1998) *Trends Neurosci.* **21,** 148–154.
4. Singer, D., Biel, M., Lotan, I., Flockerzi, V., Hofmann, F., and Dascal, N. (1991) *Science* **253,** 1553–1557.
5. Welling, A., Kwan, Y. W., Bosse, E., Flockerzi, V., Hofmann, F., and Kass, R. S. (1993) *Circ. Res.* **73,** 974–980.
6. Shistik, E., Ivanina, T., Puri, T., Hosey, M., and Dascal, N. (1995) *J. Physiol.* **489,** 55–62.
7. De Waard, M., and Campbell, K. P. (1995) *J. Physiol.* **485,** 619–634.
8. Wei, X., Pan, S., Lang, W., Kim, H., Schneider, T., Perez-Reyes, E., and Birnbaumer, L. (1995) *J. Biol. Chem.* **270,** 27106–27111.
9. Bangalore, R., Gingrich, M. K., Hofmann, F., and Kass, R. S. (1996) *Am. J. Physiol.* **270,** H1521–H1528.
10. Gurnett, C. A., Felix, R., and Campbell, K. P. (1997) *J. Biol. Chem.* **272,** 18508–18512.
11. Felix, R., Gurnett, C. A., De Waard, M., and Campbell, K. (1997) *J. Neurosci.* **17,** 6884–6891.
12. Jones, L. P., Wei, S-K., and Yue, D. T. (1998) *J. Gen. Physiol.* **112,** 125–143.
13. Mori, Y., Friedrich, T., Kim, M.-S., Mikami, A., Nakai, J., Ruth, P., Bosse, E., Hofmann, F., Flockerzi, V., Furuichi, T., Mikoshiba, K., Imoto, K., Tanabe, T., and Numa, S. (1991) *Nature* **350,** 159–162.
14. Varadi, G., Lory, P., Schultz, D., Varadi, M., and Schwartz, A. (1991) *Nature* **352,** 159–162.
15. Lacerda, A. E., Kim, H. S., Ruth, P., Perez-Reyes, E., Flockerzi, V., Hofmann, F., Birnbaumer, L., and Brown, A. M. (1991) *Nature* **352,** 527–530.
16. Perez-Reyes, E., Castellano, A., Kim, H. S., Bertrand, P., Baggstrom, E., Lacerda, A. E., Wei, X., and Birnbaumer, L. (1992) *J. Biol. Chem.* **267,** 1792–1797.
17. Neely, A., Wei, X., Olcese, R., Birnbaumer, L., and Stefani, E. (1993) *Science* **262,** 575–578.
18. Lory, P., Varadi, G., Slish, D. F., Varadi, M., and Schwartz, A. (1993) *FEBS Lett.* **315,** 167–172.
19. Nishimura, S., Takeshima, H., Hofmann, F., Flockerzi, V., and Imoto, K. (1993) *FEBS Lett.* **324,** 283–286.
20. Castellano, A., Wei, X., Birnbaumer, L., and Perez-Reyes, E. (1993) *J. Biol. Chem.* **268,** 12359–12366.
21. Wakamori, M., Mikala, G., Schwartz, A., and Yatani, A. (1993) *Biochem. Biopys. Res. Commun.* **196,** 1170–1176.
22. Mitterdorfer, J., Froschmayr, M., Grabner, M., Striessnig, J., and Glossman, H. (1994) *FEBS Lett.* **352,** 141–145.
23. Olcese, R., Qin, N., Schnider, T., Neely, A., Wei, X., Stefani, E., and Birnbaumer, L. (1994) *Neuron* **13,** 1433–1438.
24. Perez-Garcia, M. T., Kamp, T. J., and Marban, E. (1995) *J. Gen. Physiol.* **105,** 289–306.
25. Chien, A. J., Zhao, X., Shirokov, R. E., Puri, T. S., Chang, C. F., Sun, D., Rios, E., and Hosey, M. M. (1995) *J. Biol. Chem.* **270,** 30036–30044.
26. Josephson, I. R., and Varadi, G. (1996) *Biophys. J.* **70,** 1285–1293.
27. Kamp, T. J., Perez-Garcia, M. T., and Marban, E. (1996) *J. Physiol.* **492,** 89–96.
28. Olcese, R., Neely, A., Qin, N., Wei, X., Birnbaumer, L., and Stefani, E. (1996) *J. Physiol.* **497,** 675–686.
29. Brice, N. L., Berrow, N. S., Campbell, V., Page, K. M., Brickley, K., Tedder, I., and Dolphin, A. C. (1997) *Eur. J. Neurosci.* **9,** 749–759.
30. Tareilus, E., Roux, M., Qin, N., Olcese, R., Zhou, J., Stefani, E., and Birnbaumer, L. (1997) *Proc. Natl. Acad. Sci. USA* **94,** 1703–1708.
31. Constantin, J., Noceti, F., Qin, N., Wei, X., Birnbaumer, L., and Stefani, E. (1998) *J. Physiol.* **507,** 93–103.
32. Yamaguchi, H., Hara, M., Strobeck, M., Fukasawa, K., Schwartz, A., and Varadi, G. (1998) *J. Biol. Chem.* **273,** 19348–19356.
33. Gao, T., Chien, A. J., and Hosey, M. M. (1999) *J. Biol. Chem.* **274,** 2137–2144.
34. Shistik, E., Ivanina, T., Blumenstein, Y., and Dascal, N. (1998) *J. Biol. Chem.* **273,** 17901–17909.
35. Rios, E., and Brum, G. (1987) *Nature* **325,** 717–720.
36. Hadley, R. W., and Lederer, W. J. (1992) *Am. J. Physiol.* **262,** H472–H477.
37. Allen, T. J. A., and Mikala, G. (1998) *Pflügers Arch.* **436,** 238–247.
38. Schultz, D., Mikala, G., Yatani, A., Engle, D. B., Iles, D. E., Segers, B., Sinke, R. J., Weghuis, D. O., Klöckner, U., Wakamori,

M., Wang, J., Melvin, D., Varadi, G., and Schwartz, A. (1993) *Proc. Natl. Acad. Sci. USA* **90,** 6228–6232.

39. Ellis, S. B., Williams, M. E., Ways, N. R., Brenner, R., Sharp, A., Leung, A. T., Campbell, K. P., McKenna, E., Koch, W. J., Hui, A., Schwartz, A., and Harpold, M. M. (1988) *Science* **241,** 1661–1664.
40. Yamaguchi, H., Muth, J. N., Varadi, M., Schwartz, A., and Varadi, G. (1999) *Proc. Natl. Acad. Sci. USA* **96,** 1357–1362.
41. Qin, N., Platano, D., Olcese, R., Costantin, J. L., Stefani, E., and Birnbaumer, L. (1998) *Proc. Natl. Acad. Sci. USA* **95,** 4690–4695.
42. Bichet, D., Cornet, V., Carlier, E., Geib, S., Volsen, S., Hoshi, T., and De Waard, M. (1999) *Biophys. J.* **76,** A91.
43. Birnbaumer, L., Qin, N., Olcese, R., Tareilus, E., Platano, D., Constantin, J. L., and Stefani, E. (1998) *J. Bioenerg. Biomembr.* **30,** 357–375.
44. Hullin, R., Singer-Lahat, D., Friechel, M., Biel, M., Dascal, N., Hofmann, F., and Flockerzi, V. (1992) *EMBO J.* **11,** 885–890.
45. Massa, E., Kelly, K. M., Yule, D. I., MacDonald, R. L., and Uhler, M. D. (1995) *Mol. Pharmacol.* **47,** 707–716.